Carbohydrate Polymers 115 (2015) 525–532

Contents lists available at ScienceDirect

Carbohydrate Polymers

journal homepage: www.elsevier.com/locate/carbpol

Use of gum arabic to improve the fabrication of chitosan–gelatin-based nanofibers for tissue engineering

Ruei-Yi Tsai[a], Ting-Yun Kuo[a], Shih-Chieh Hung[b,c], Che-Min Lin[a], Tzu-Yang Hsien[d], Da-Ming Wang[a], Hsyue-Jen Hsieh[a,*]

[a] Department of Chemical Engineering, National Taiwan University, Taipei 106, Taiwan
[b] Department of Orthopedics and Traumatology, Taipei Veterans General Hospital, Taipei 112, Taiwan
[c] Faculty of Medicine, Institute of Clinical Medicine, National Yang-Ming University, Taipei 112, Taiwan
[d] General Education Center, China University of Technology, Taipei 116, Taiwan

ARTICLE INFO

Article history:
Received 25 April 2014
Received in revised form 22 August 2014
Accepted 23 August 2014
Available online 18 September 2014

Keywords:
Electrospinning
Chitosan
Gelatin
Gum arabic
Viscosity
Cytocompatibility

ABSTRACT

Current techniques for fabricating chitosan–gelatin-based nanofibers require the use of corrosive and expensive solvents. Our novel method, however, using gum arabic and a mild (20 wt%) aqueous acetic acid solution as solvent can produce a solution with much higher chitosan–gelatin content (16 wt%). Without gum arabic, which greatly decreases the viscosity of the solution, such an outcome was unachievable. The solution was utilized to prepare electrospun chitosan–gelatin–polyvinyl alcohol–gum arabic nanofibers with a weight ratio of 8:8:2:0.5 (C8G8P2A0.5 nanofibers), in which polyvinyl alcohol could stabilize the electrospinning process. The stability and tensile strength (2.53 MPa) of C8G8P2A0.5 nanofibers (mats) were enhanced by glutaraldehyde crosslinking. Furthermore, mesenchymal stem cells attached and proliferated well on the mat. The strength-enhanced and cytocompatible C8G8P2A0.5 mats are thereby suitable for tissue engineering applications. More importantly, we have created a less expensive and safer method (one not using hazardous solvents) to fabricate chitosan–gelatin-based nanofibers.

1. Introduction

Electrospinning is a relatively simple and effective technique in which applied electrostatic force is used to overcome the surface tension of a solution containing candidate materials to produce fibers with diameters ranging from several nanometers to micrometers (Doshi & Reneker, 1995; Huang, Zhang, Kotaki, & Ramakrishna, 2003; Kiechel & Schauer, 2013; Reneker & Chun, 1996). These fibers are structurally similar to the extracellular matrix (ECM) and are thus regarded as potential materials for tissue engineering. The morphology of fibers is affected by many parameters, including solution properties, processing parameters, and ambient conditions (Deitzel, Kleinmeyer, Harris, & Tan, 2001; Haghi & Akbari, 2007; Hohman, Shin, Rutledge, & Brenner, 2001; Yuan, Zhang, Dong, & Sheng, 2004; Zong et al., 2002). Among these parameters, the viscosity of the solution plays a crucial role in the electrospinning process.

Industrial chitosan, the cationic (1-4)-2-amino-2-deoxy-β-D-glucan, has a typical degree of acetylation close to 20%. It is produced from fishery by-products (Muzzarelli, 1977, 2012; Muzzarelli et al., 2012). Chitosan is soluble in acidic solution by protonation of amino groups and thus is positively charged. In addition, the formation of hydrogen bonds leads to a dramatic increase in the viscosity of chitosan solution at high concentration (Desbrieres, 2002). Chitosan is often used in tissue engineering due to its non-toxicity, growth factor-stabilizing effect, and other favorable properties (Busilacchi, Gigante, Mattioli-Belmonte, Manzotti, & Muzzarelli, 2013; Muzzarelli, 2011). For preparing chitosan fibers by electrospinning, the concentration of chitosan solution should be above a certain level for proper molecular entanglement to occur. At high concentrations, however, chitosan solution becomes highly viscous and cannot flow through the syringe needle in the electrospinning process. This impediment hinders the production of fibers (Shenoy, Bates, Frisch, & Wnek, 2005). Some researchers have prepared electrospun chitosan-based fibers by blending chitosan with a large amount of water-soluble polymers, such as polyvinyl alcohol (PVA) or polyethylene oxide (PEO), to decrease the viscosity of the solution (Huang, Zhang, Ramakrishna, & Lim, 2004; Kidoaki, Kwon, & Matsuda, 2005). Alternatively, electrospun pure chitosan fibers can be fabricated by using trifluoroacetic acid (TFA) or hexafluoroisopropanol (HFIP) as a solvent (Chen, Wang, Wei, Mo, & Cui, 2010; Nam, Park, Ihm, & Hudson, 2010; Schiffman

* Corresponding author. Tel.: +886 2 23633097; fax: +886 2 23623040.
E-mail address: hjhsieh@ntu.edu.tw (H.-J. Hsieh).

http://dx.doi.org/10.1016/j.carbpol.2014.08.108
0144-8617/

& Schauer, 2007). However, TFA and HFIP are highly corrosive and quite expensive. Geng, Kwon, and Jang (2005) reported that chitosan (7 wt%) with a molecular weight of 106 kDa dissolved in 90% aqueous acetic acid exhibited a suitable viscosity and could be fabricated into fibers by electrospinning. In a later study, chitosan was blended with gelatin to improve the cytocompatibility of the electrospun mat (Zhu, Cui, Li, & Jin, 2008). Gelatin, a natural water-soluble polymer derived from partial hydrolysis of collagen, possesses an arginine–glycine–aspartic acid (RGD) peptide sequence and is widely used as a biomaterial for tissue engineering applications (Ma, He, Yong, & Ramakrishna, 2005; Rosellini, Cristallini, Barbani, Vozzi, & Giusti, 2009).

Gum arabic is a highly branched polysaccharide consisting of a β-(1-3) galactose backbone with linked branches of arabinose, rhamnose, and glucuronic acid (Swenson, Kaustine, Kaustine, & Thompson, 1968). The highly branched structure causes a relatively small hydrodynamic volume, which decreases the intermolecular interaction between gum arabic molecules (Phillips & Williams, 2000). Our newly published article indicates that chitosan and gum arabic form a globe-like microstructure with an inner core consisting of gum arabic/chitosan and an outer part mostly consisting of chitosan (Tsai et al., 2014). This microstructure strongly decreases the viscosity of chitosan solution (Tsai et al., 2014). In the present study, the viscosity-decreasing effect of gum arabic was utilized to improve the electrospinning of viscous chitosan-based solution into fibers. To the best of our knowledge, gum arabic has not yet been utilized in the electrospinning process of chitosan. Therefore, our study was the first attempt to produce electrospun chitosan-based nanofibers using gum arabic.

To improve cell attachment and cytocompatibility, the content of chitosan and gelatin in the nanofibers for tissue engineering needs to be increased. As mentioned earlier, current techniques for fabricating electrospun nanofibers with high chitosan and gelatin content require the use of corrosive and/or expensive solvent, such as TFA or HFIP. The purpose of this study was to create a safer and less expensive method to prepare chitosan–gelatin-based nanofibers. This purpose was achieved by using gum arabic (a viscosity-decreasing agent) and an aqueous acetic acid solution as solvent to produce a solution with much higher chitosan–gelatin content (16 wt%). The solution was electrospun into chitosan–gelatin-rich nanofibers with suitable cytocompatibility for tissue engineering applications.

2. Materials and methods

2.1. Materials

Chitosan with a molecular weight of about 300 kDa and degree of deacetylation of 90% was purchased from Kiotek (Taipei, Taiwan). Gelatin (G9391) and gum arabic (G9752, branched polysaccharide from acacia tree) were purchased from Sigma-Aldrich (St. Louis, USA). Polyvinyl alcohol (PVA) (M.W. 75 kDa) was supplied by Chang Chun Petrochemical Co. Ltd (Taiwan). All other solvents and chemicals were of reagent grade.

2.2. Viscosity measurement

Gum arabic powder was dissolved in deionized water, and then chitosan powder was added to the solution with gentle stirring. After uniform dispersion of the chitosan powder, acetic acid (final concentration: 20 wt%) was added to dissolve the chitosan to produce a series of mixed solutions of chitosan (C) and gum arabic (A) called C*x*A*y* solutions, where *x* and *y* denote the wt% of chitosan and gum arabic, respectively. The C*x*A*y* solutions were classified into three groups namely A0, A0.5, and A1 groups according to the wt% of gum Arabic. The A0 group included C1A0, C2A0, C3A0, C4A0, C5A0, and C6A0 solutions, i.e., pure chitosan (1–6 wt%) solutions. The A0.5 group included C4A0.5, C6A0.5, C8A0.5, C10A0.5, C12A0.5, C14A0.5 and C16A0.5 solutions, i.e., chitosan–gum arabic hybrid solutions containing various concentrations of chitosan (4–16 wt%) and 0.5 wt% gum arabic. The A1 group included C4A1, C6A1, C8A1, C10A1, C12A1, C14A1 and C16A1 solutions, i.e., chitosan–gum arabic hybrid solutions containing various concentrations of chitosan (4–16 wt%) and 1 wt% gum arabic. Subsequently, the viscosities of various C*x*A*y* solutions were measured by using a viscometer (model DV-II+, Brookfield, USA) at a rotational speed of 1.5 rpm.

2.3. Electrospinning of hybrid nanofibers

Chitosan (C), gelatin (G), PVA (P), and gum arabic (A) were used to prepare two types of hybrid solutions containing C/G/A or C/G/P/A plus 20 wt% acetic acid, as shown in Table 1. These solutions were utilized to fabricate hybrid nanofibers using an electrospinning unit (Jyi-Goang Enterprise, Taipei, Taiwan). The hybrid solution was loaded in a 3 mL syringe and fed at a flow rate of 0.15–0.3 mL/h by a syringe pump. A high electric voltage (15–30 kV) was applied between a 23 G needle and a vertical collector at a distance of 15 cm. The environmental temperature and relative humidity were controlled at 30 °C and 40%, respectively. The resultant nanofibers were carefully removed from the collector for further treatment and characterization. The thickness of the electrospun nanofibers (mat) was quite uniform (about 100 μm) and each mat was measured three times by a micrometer caliper.

2.4. Morphology of nanofibers

The electrospun nanofibers were dried in a vacuum oven (HDOV-30, Deng Yng, Taiwan) for 3 h at 40 °C. After the fibers were sputter-coated with platinum, their morphology was observed using a scanning electron microscope (SEM, Nova NanoSEM 230, USA). The working voltage and distance for the SEM were 5 kV and 5 mm, respectively. The diameters of 100 nanofibers were measured from high-magnification micrographs and a histogram of fiber diameter distribution was constructed.

2.5. Porosity of electrospun mats

The electrospun C8G8P2A0.5 mats were dried in a vacuum oven. The density of each mat (ρ_m) was determined from the overall mass divided by the volume of the mat. The average bulk density (ρ_0) of constituent polymers was calculated from the bulk densities of C, G, P, and A multiplied by their respective mass fractions. According to the on-line MSDS information (http://www.sciencelab.com/), the bulk densities of C, G, P, and A are 1.4, 1.2, 1.25, and 1.425, respectively. The porosity of the mats was calculated by using the following equation (Wang, Fang, Yoon, Hsiao, & Chu, 2006):

$$\text{porosity} = \left(1 - \frac{\rho_m}{\rho_0}\right) \times 100\%$$

2.6. Stability of crosslinked mats

The electrospun C8G8P2A0.5 mats were crosslinked with glutaraldehyde vapor for 0, 6, 12, and 24 h (termed GA0, GA6, GA12 and GA24) to enhance its stability. After vacuum drying overnight, the initial dry weight of each mat (W_i) was measured. The electrospun mats were then immersed in phosphate buffered saline (PBS) with shaking at 37 °C. After 1, 3, 7, and 14 days of incubation, the mats were vacuum-dried overnight again and the residual dry weight (W_f) was measured. The remaining weight percentage was

Table 1
Symbols and compositions of the two types of hybrid solutions containing C/G/A or C/G/P/A plus 20 wt% acetic acid, where C, G, P, and A denote chitosan, gelatin, PVA, and gum arabic, respectively.

Symbols	Type	(Unit: g)						
		Chitosan (C)	Gelatin (G)	PVA (P)	Gum arabic (A)	Acetic acid	Water	Total
C8G8A0.5	C/G/A	8	8	0	0.5	20	63.5	100
C8G8P2A0.5	C/G/P/A	8	8	2	0.5	20	61.5	100

used as an index of the stability of the mats in aqueous environment and calculated using the following formula:

$$\text{Remainin weight percentage } (\%) = \frac{W_f}{W_i} \times 100\%$$

2.7. Mechanical properties of mats

The electrospun mats were cut into a dog-bone shape, and the tensile strength (stress at maximum load) and elongation of the mats were measured with a tensile strength instrument (model LRX, Lloyd, Hampshire, UK) at a stretching rate of 10 mm/min.

2.8. Permeability of mats

To characterize the permeation of large molecule such as bovine serum albumin (BSA) through the mat, side-by-side diffusion cells were used. An electrospun C8G8P2A0.5 mat was mounted as a barrier between the donor cell and the receptor cell. Then 20 mL BSA solution (PBS containing 4 mg BSA) was loaded into the donor cell, and another 20 mL solution containing only PBS was loaded into the receptor cell, with both cells under stirring. At pre-designated time points, the concentrations of BSA in both cells were sampled and determined. The initial permeability (P_i) of BSA through the mat was estimated with the following formula (Baker, 1987):

$$P_i = \frac{L}{\Delta C_0}\frac{V_R}{A} \times \frac{dC_R}{dt}$$

where L is the thickness of mat, V_R is the volume of BSA solution in the receptor cell, C_R is the BSA concentration in receptor cell, ΔC_0 is the initial difference in BSA concentration between donor and receptor cells, A is the mat area used for permeation, and t is the permeation time. dC_R/dt was calculated from the initial linear section of curve C_R vs. t.

In addition, the permeability of the mat (P_t) at every sampling time interval was estimated by using the following formula:

$$P_t = \frac{L}{\Delta C_t}\frac{V_R}{A} \times \frac{\Delta C_R}{\Delta t}$$

where ΔC_t is the BSA concentration difference between donor and receptor cells at sampling time t, and ΔC_R is the difference in BSA concentration in the receptor cell at time t and $t + \Delta t$. Therefore, all P_t values could be used to find the average permeability of the mat ($\bar{P}$).

2.9. Culture of mesenchymal stem cells

Human mesenchymal stem cells (MSCs) (Hung et al., 2004) were provided by Prof. Shih-Chieh Hung (Taipei Veterans General Hospital and National Yang-Ming University). These studies were approved by the Institutional Review Board of Taipei Veterans General Hospital (2010110171C), with informed consent obtained from donors who provided bone marrow aspirates. The primary MSCs were isolated as previously described (Tsai, Su, Huang, Yew, & Hung, 2012). The immortalized MSCs (called KP-hMSCs) were developed as previously reported (Hung et al., 2004). When subjected to specific stimulating conditions in vitro, KP-hMSCs could respond and differentiate along the mesenchymal (bone, fat and cartilage) and nonmesenchymal (neuron) cell lineages (Hung et al., 2004). KP-hMSCs were cultured in Dulbecco's modified Eagle's medium-low glucose (LG-DMEM) containing 10% fetal bovine serum (FBS) and 1% antibiotics in a 5% CO_2/95% air incubator with saturated humidity at 37 °C. As the cell density reached about 90% confluence, the cells were harvested and then seeded onto the various surfaces (including dense film, electrospun mat, and TCPS) at a seeding density of 3×10^4 cells per sample (size: 3.8 cm^2). On days 1, 3, 5, and 7, the total amount of cellular proteins of KP-hMSCs was measured with a Micro BCA™ Protein Assay Kit (Thermo Scientific, USA) to reveal the cell number. The total protein assay was done using a 96-well microplate reader (BioTek, USA) with a wavelength of 570 nm.

2.10. Observation of cell morphology

The live-dead fluorescent stain was utilized to reveal the attachment and morphology of KP-hMSCs on various surfaces. Fluorescein diacetate (FDA, 10 μg/mL) and propidium iodide (PI, 5 μg/mL) were prepared in LG-DMEM and incubated with KP-hMSCs for 10 min. Then the FDA- & PI-containing medium was replaced by fresh LG-DMEM. The live and dead cells fluoresced green and red, respectively under a fluorescence microscope (IX70-S8F, Olympus, Japan). The excitation/emission wavelengths are 490 nm/535 nm for FDA and 490 nm/610 nm for PI (Bernardi, Scorrano, Colonna, Petronilli, & Di Lisa, 1999). Furthermore, the cells on the C8G8P2A0.5 mat were fixed by 2.5% glutaraldehyde prepared in PBS for 3 h at 4 °C. After being washed 3 times with PBS, dehydrated step-by-step with 30%, 50%, 60%, 70%, 80%, 90%, 95% and 100% ethanol solution (each step 15 min), critical point dried for 30 min, and sputter-coated with platinum, the samples were observed by SEM.

2.11. Statistical analysis

All data are expressed as the mean values ± standard deviation. Mean separations were determined using the Student's t test with a level of significance of $P < 0.05$.

3. Results and discussion

3.1. Viscosity of chitosan–gum arabic hybrid solution

As we have shown recently, the chitosan–gum arabic hybrid solution with a total concentration of 1 wt% exhibits a low viscosity due to the formation of the globe-like microstructure (Tsai et al., 2014). In this study, chitosan–gum arabic hybrid solutions (CxAy solutions, where x and y denote the wt% of chitosan and gum arabic, respectively.) with higher concentrations of both components were prepared. Fig. 1 shows the viscosity of pure chitosan (1–6 wt%) solution (A0 group) and chitosan–gum arabic hybrid solutions containing various concentrations of chitosan (4–16 wt%) and either 0.5 wt% gum arabic (A0.5 group) or 1 wt% gum arabic (A1 group) using a 20 wt% aqueous acetic acid solution as a solvent. (See Section 2.2 for a complete listing of the samples prepared.) The viscosity of pure chitosan solution (curve A0) increased rapidly with concentration (especially above 4 wt%), increasing from 4840 cP to 17110 cP

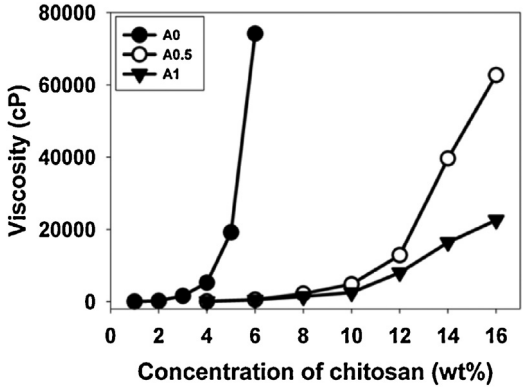

Fig. 1. Viscosity of pure chitosan solution (A0) and chitosan–gum arabic hybrid solution containing 0.5 wt% (A0.5) and 1 wt% (A1) gum arabic at various concentrations of chitosan. The solutions were prepared using a 20 wt% aqueous acetic acid solution as a solvent. The viscosity was measured at a rotational speed of 1.5 rpm.

and 74180 cP for the C4A0, C5A0, and C6A0 chitosan–gum arabic hybrid solutions, respectively (Fig. 1). In contrast, after the addition of 0.5 wt% gum arabic, the viscosity of chitosan–gum arabic hybrid solution (curve A0.5) increased only slightly with increasing chitosan concentration when the concentration was below 10 wt%. The viscosity of the C10A0.5 solution was still below 5000 cP. When the chitosan concentration was higher than 12 wt%, the viscosity of the hybrid solution started to increase significantly. However, the viscosity of a highly concentrated hybrid solution such as C16A0.5 solution (62740 cP) was still lower than that of C6A0 solution, clearly indicating that the addition of gum arabic greatly decreased the viscosity of the solution. Increasing the amount of gum arabic to 1 wt%, as expected, further decreased the viscosity of the hybrid solution (curve A1). The viscosity of C16A1 solution was only 22580 cP, considerably lower than that of C16A0.5 solution (62740 cP), as mentioned above.

Electrospinning of chitosan with a high molecular weight is difficult if aqueous acetic acid solution is utilized as a solvent because the resultant solution is highly viscous and thus not suitable for electrospinning. Fig. 1 shows that a chitosan-based solution becomes much less viscous when gum arabic is added. Therefore, the concentration of chitosan can be further increased and more molecular entanglements may form, which then enhance the fabrication of chitosan-based nanofibers by electrospinning. Our unpublished data suggest that electrospun chitosan-based hybrid nanofibers can be produced from a hybrid solution with a viscosity ranging from about 3500 to 5000 cP (prepared in 20 wt% acetic acid solution). Based on this criterion, we thought that the use of 0.5 wt% gum arabic in hybrid solution would be appropriate and that consequently, the concentration of chitosan could be increased significantly to 8 wt% (Fig. 1). In addition, gelatin can be added to the hybrid solution to improve the cytocompatibility of electrospun nanofibers (Le Trong, McDevitt, Nelson, Stayton, & Stenkamp, 2003). Therefore, we proposed a reasonable composition for preparing the hybrid solution, one in which the concentrations of chitosan, gelatin, and gum arabic were 8 wt%, 8 wt%, and 0.5 wt%, respectively (termed C8G8A0.5 solution). This solution was utilized to prepare electrospun C8G8A0.5 nanofibers (with high chitosan–gelatin content) in the following experiments for further analysis.

3.2. Morphology of C8G8A0.5 and C8G8P2A0.5 nanofibers

The morphology and diameter of electrospun nanofibers are influenced by many parameters, including applied voltage, flow

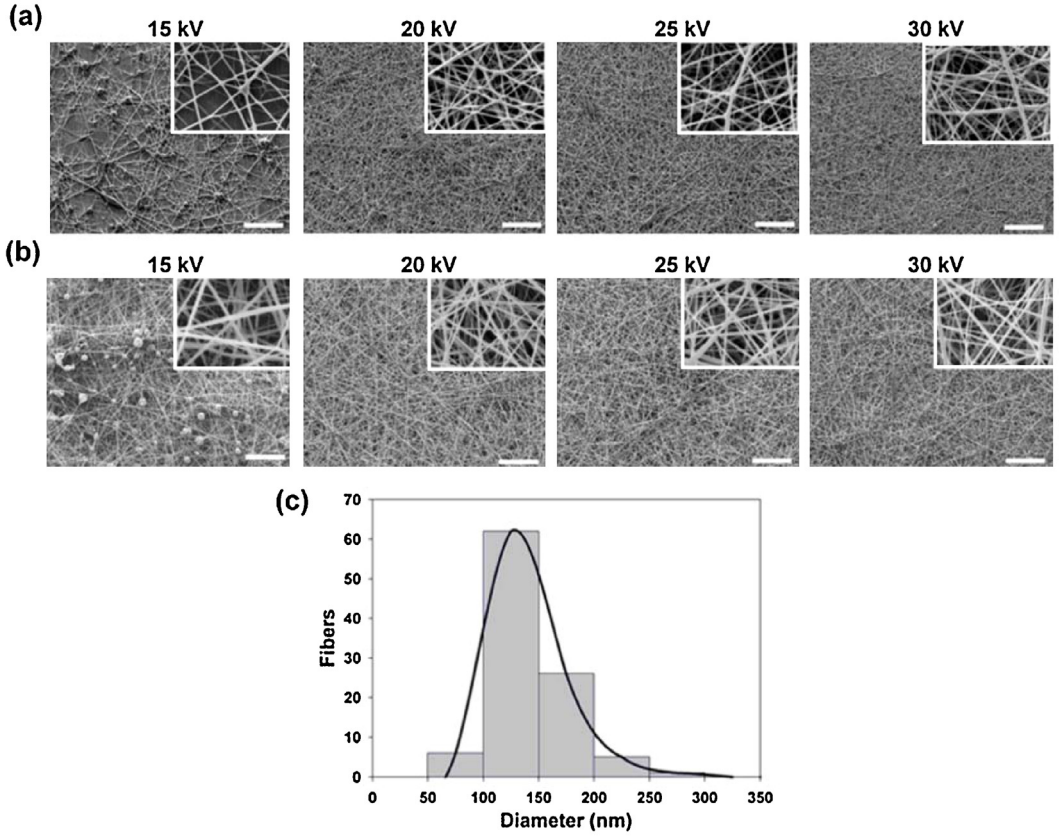

Fig. 2. SEM micrographs of the electrospun (a) C8G8A0.5 and (b) C8G8P2A0.5 nanofibers prepared at various applied voltages. Scale bars and the widths of small images are both 10 μm. (c) The diameter distribution of the electrospun C8G8P2A0.5 nanofibers prepared at an applied voltage of 25 kV and a flow rate of 0.3 mL/h.

rate, solution viscosity, and working distance. Fig. 2(a) shows SEM micrographs of electrospun chitosan–gelatin–gum arabic (C8G8A0.5) nanofibers produced at various applied voltages and flow rates with a constant working distance of 15 cm. When the applied voltage was higher than 20 kV, uniform and defect-free nanofibers were produced by electrospinning, clearly indicating that the molecular entanglements in C8G8A0.5 hybrid solution and the viscosity of the solution were suitable for electrospinning.

However, we found that the electrospinning jet gradually became unstable as time elapsed. To maintain a stable electrospinning jet, a small amount of PVA (2 wt%) was added to assist the formation of nanofibers. The proportion of PVA to overall polymers was only about 10%. Fig. 2(b) shows SEM micrographs of the resultant electrospun chitosan–gelatin–PVA–gum arabic (termed C8G8P2A0.5) nanofibers produced at various applied voltages and flow rates. In comparison to C8G8A0.5 nanofibers (Fig. 2(a)), more C8G8P2A0.5 nanofibers could be collected at a lower applied voltage (15 kV) and the nanofibers thus produced were more uniform. Most importantly, a stable Taylor cone of the electrospinning jet could be maintained, so the electrospun C8G8P2A0.5 nanofibers were produced steadily at an applied voltage of 20–25 kV and a flow rate of 0.3 mL/h for a prolonged period of time. Therefore, electrospun C8G8P2A0.5 nanofibrous mats (with high chitosan–gelatin content) were used in the following analyses.

3.3. Diameter distribution and porosity of nanofibrous mats

Electrospun C8G8P2A0.5 nanofibrous mats prepared at an applied voltage of 25 kV and a flow rate of 0.3 mL/h were subjected to SEM analysis. The average diameter of C8G8P2A0.5 nanofibers was 143 ± 31 nm (determined by measuring 100 nanofibers on the SEM micrograph), and the distribution of fiber diameters is shown in Fig. 2(c). Most nanofibers were in the range of 100–200 nm.

In addition, the electrospun C8G8P2A0.5 nanofibrous mat was highly porous, having a porosity of 87–90%. However, the pore size (about 2–3 μm) of the mat was still too small for cell infiltration. Therefore, in the subsequent cytocompatibility test, the cells would stay on the surface of the mat instead of infiltrating into the mat.

3.4. Stability of crosslinked mats in aqueous solution

In order to improve the stability and mechanical properties, the electrospun C8G8P2A0.5 nanofibrous mat was crosslinked with glutaraldehyde (GA) vapor for 0–24 h. The mat was then soaked in PBS buffer for 14 days, and the remaining weight percentage of the mat was used to represent its stability, as shown in Fig. 3(a). The uncrosslinked mat (GA0) lost about 55% of its initial weight in the first 3 days and then remained almost unchanged until the last day. However, in the case of the mats crosslinked with glutaraldehyde vapor for 6 h (GA6), 12 h (GA12), and 24 h (GA24), their remaining weight percentages at the end of the 14 days of immersion were 75%, 82%, and 93%, respectively. It was clear that the increasing the crosslinking time increased the stability of the mat. The morphologies of uncrosslinked and crosslinked C8G8P2A0.5 nanofibrous mats soaked in PBS for 3 days are shown in Fig. 3(b). The uncrosslinked mat (GA0) became flattened and the nanofibers fused together. The 6 h crosslinked mat (GA6) maintained the fibrous structure, but the nanofibers exhibited slight distortion. Better morphologies and more stable structures were found in the 12 h crosslinked mat (GA12) and the 24 h crosslinked mat (GA24) (Fig. 3(b)). Based on these results, it was evident that water-soluble polymers such as gelatin and PVA could be crosslinked with glutaraldehyde vapor and the fibrous structure and morphology of the crosslinked mats thereby preserved (Jegal & Lee, 1999).

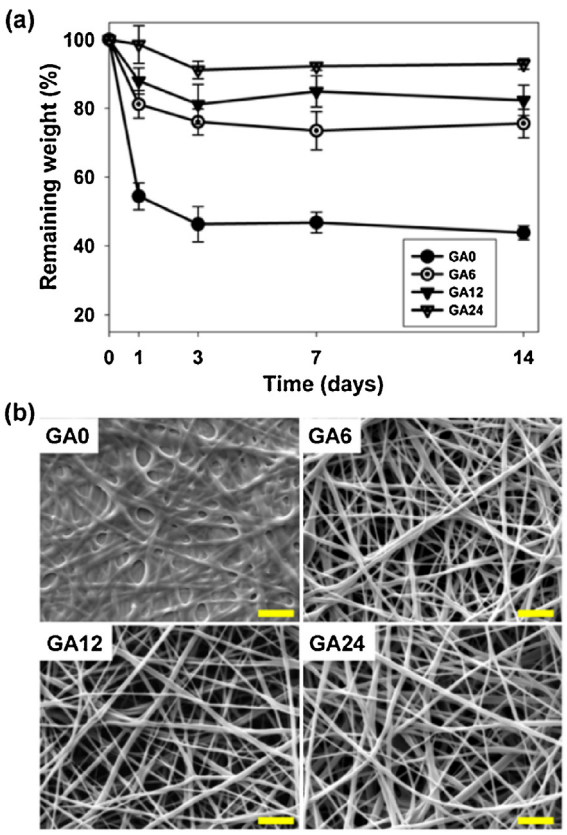

Fig. 3. (a) Stability (represented by the remaining weight percentage) of C8G8P2A0.5 mat immersed in PBS for 0–14 days, and (b) SEM micrographs of C8G8P2A0.5 mat after 3 days of immersion in PBS. The C8G8P2A0.5 mat was uncrosslinked (GA0) or crosslinked with glutaraldehyde vapor for 6 h (GA6), 12 h (GA12), and 24 h (GA24).

3.5. Mechanical properties of mats

Fig. 4 shows the tensile strengths (stress at the maximum load) and elongation capabilities of the uncrosslinked mat (GA0), 12 h crosslinked mat (GA12), and 24 h crosslinked mat (GA24). The GA12 mat exhibited the highest tensile strength, which was about 4 times that of the GA0 mat (2.53 ± 0.22 vs. 0.67 ± 0.15 MPa). Prolonging the crosslinking time to 24 h did not further increase the tensile strength of the GA24 mat. As for the elongation capability, as expected, the GA0 mat exhibited a relatively higher elongation percentage. Based on the results of the stability and mechanical property analyses, we chose to use the 12-h crosslinked C8G8P2A0.5 mat in the following evaluations of permeability and cytocompatibility.

3.6. Permeability of crosslinked mats

The permeation of large molecules (BSA protein molecules) through the electrospun C8G8P2A0.5 mat crosslinked for 12 h was investigated using side-by-side diffusion cells. As time elapsed, variations in BSA contents in the donor and receptor cells (both having the same volume) were measured, and then the corresponding permeation characteristics (flux and permeability) of BSA through the mat were determined, as shown in Fig. 5. In the beginning, small amounts of BSA were adsorbed on the mat, which caused the contents in the donor cell to decrease fast, but in the receptor cell, the contents increased more slowly. Eventually, the BSA contents in the donor and receptor cells reached equilibrium.

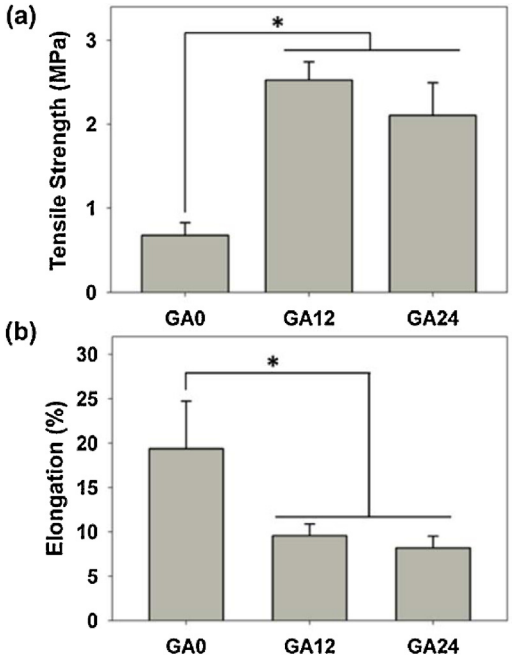

Fig. 4. (a) Tensile strength (stress at the maximum load) and (b) elongation capability of C8G8P2A0.5 mat uncrosslinked (GA0) or crosslinked with glutaraldehyde vapor for 12 h (GA12), and 24 h (GA24). * $P < 0.05$.

As shown in Fig. 5(a), about 10% of BSA molecules adsorbed on the mat in the first 3 h, so the BSA content in the donor cell decreased rapidly while that in the receptor cell increased only gradually. It took 168 h for the BSA contents (concentrations) in the donor and receptor cells to become almost equal. Linear least squares regression based on the data (0–12 h) from

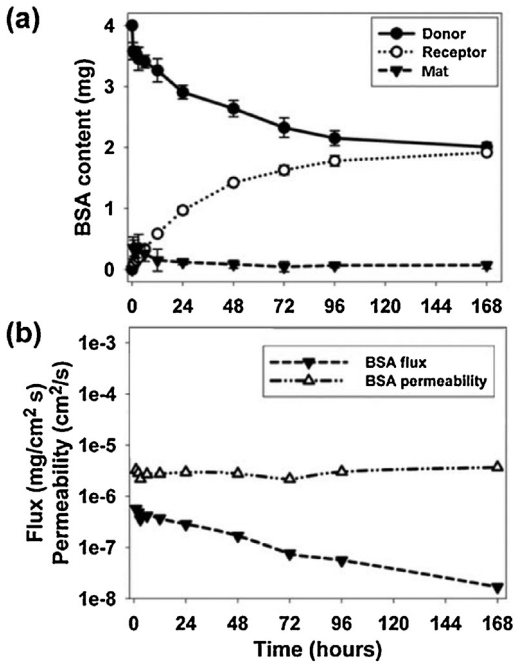

Fig. 5. The permeation of BSA protein molecules through the crosslinked C8G8P2A0.5 mat in side-by-side diffusion cells. (a) BSA contents in the donor and receptor cells and those adsorbed on the mat at different time points were determined, and then those contents were used to calculate (b) the flux and permeability values of BSA molecules through the mat.

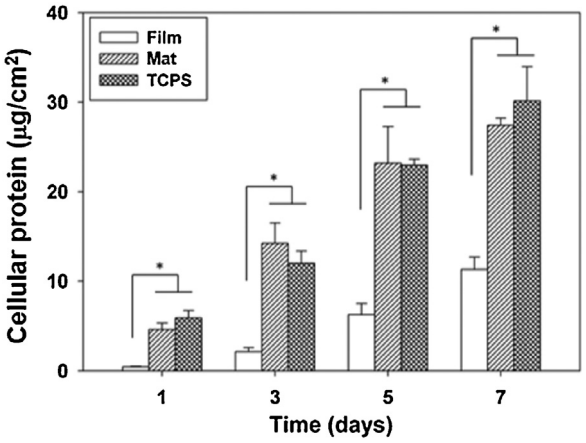

Fig. 6. Proliferation of KP-hMSCs cultured on C8G8P2A0.5 film, C8G8P2A0.5 mat, and TCPS for 1 to 7 days. The total cellular protein densities were measured to indicate the cell densities of KP-hMSCs implicitly. * $P < 0.05$.

Fig. 5(a) indicated that the initial permeability value of BSA was 1.70×10^{-6} cm^2/s.

For more detailed analysis of the permeation behavior of BSA, the flux and permeability value in each time interval were calculated, as shown in Fig. 5(b). The permeability value of BSA exhibited an initial drop due to the adsorption of BSA on the mat, followed by a gradual increase to a relatively stable range. The average permeability value for BSA (during 0–168 h) was 2.83×10^{-6} cm^2/s, which was obviously higher than the corresponding initial permeability value (i.e., 1.70×10^{-6} cm^2/s) because of the initial adsorption. Therefore, even for large molecules like BSA, the permeability value was quite stable for 168 h (7 days), indicating that the electrospun C8G8P2A0.5 mat allowed large molecules to permeate steadily.

3.7. Cytocompatibility of electrospun C8G8P2A0.5 mat

For the cytocompatibility test, we chose the 12-h crosslinked electrospun C8G8P2A0.5 mat as a promising biomaterial, and we used a dense C8G8P2A0.5 film and a tissue culture polystyrene (TCPS) surface for comparison. For this test, the mesenchymal stem cells (KP-hMSCs) were cultured on these three surfaces (film, mat, and TCPS) and the corresponding proliferation of KP-hMSCs with time was determined, as shown in Fig. 6. On days 1, 3, 5, and 7, the total cellular protein densities (representing the cell densities of KP-hMSCs implicitly) on the mat and TCPS surfaces were significantly higher than that on the dense film. On day 7, the cellular protein densities on the mat and TCPS surfaces were both around 30 μg/cm^2, which was about 2.5 times that on the dense film (12 μg/cm^2).

These results were further supported by the live-dead fluorescent stain using FDA and PI, as shown in Fig. 6(a). The KP-hMSCs attached and proliferated well on the mat and TCPS surfaces during the 7-day cultivation. In contrast, the KP-hMSCs formed aggregates and did not proliferate well on the dense film, possibly because for KP-hMSCs, the cell–cell interaction may be stronger than the interaction between the cell and the dense film. Fig. 7(b) shows SEM micrographs of KP-hMSCs on the nanofibrous C8G8P2A0.5 mat during the 7-day cultivation. These micrographs show that a KP-hMSC monolayer almost completely covered the mat on day 7. However, no KP-hMSC infiltration into the mat is visible because the KP-hMSCs were larger than the pores of the nanofibrous mat. In brief, our data indicated that the C8G8P2A0.5 nanofibrous mat was suitable for the attachment and proliferation of KP-hMSCs, possibly because the morphology and structure of nonwoven electrospun nanofibers were similar to that of extracellular matrix

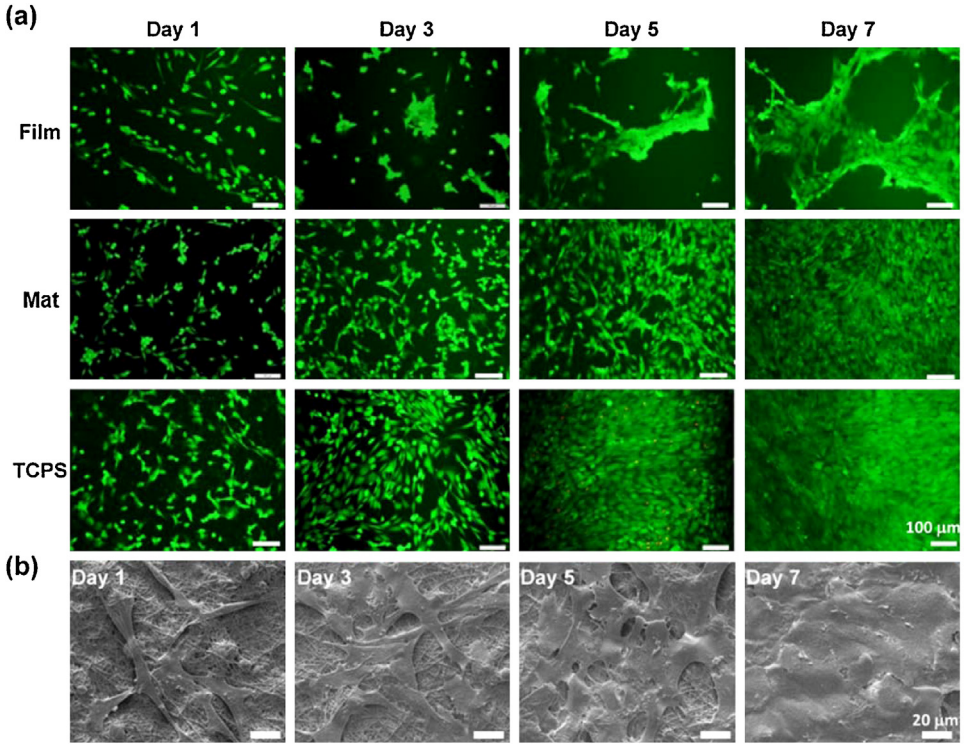

Fig. 7. (a) FDA/PI fluorescent micrographs of KP-hMSCs cultured on C8G8P2A0.5 film, C8G8P2A0.5 mat, and TCPS for 1 to 7 days. Scale bar = 100 μm. (b) SEM micrographs of KP-hMSCs cultured on the C8G8P2A0.5 mat for 1 to 7 days. Scale bar = 20 μm.

(Zhu et al., 2008) and the nanofibers had a high chitosan–gelatin content (>80%), thus rendering the electrospun C8G8P2A0.5 mat quite cytocompatible.

4. Conclusions

The use of gum arabic greatly improved the fabrication of electrospun hybrid nanofibers with high chitosan–gelatin content (>80%). Our novel method requires the use of only a mild (20 wt%) aqueous acetic acid solution as a solvent for preparing a solution with much higher chitosan–gelatin content (16 wt%) for electrospinning, which is unattainable without the addition of gum arabic to decrease the viscosity of the solution. Electrospun chitosan–gelatin–polyvinyl alcohol–gum arabic nanofibers with a component weight ratio of 8:8:2:0.5 (C8G8P2A0.5 nanofibers) were successfully produced. The stability and tensile strength of the C8G8P2A0.5 nanofibrous mat were both enhanced by 12 h of crosslinking with glutaraldehyde vapor. Permeation tests indicated that the C8G8P2A0.5 mat allowed large molecules to permeate steadily. Cytocompatibility tests using the stem cells (KP-hMSCs) revealed excellent cell attachment and proliferation on the mat. These promising results indicate that we have developed a less expensive and safer method (one not using expensive and hazardous solvents such as trifluoroacetic acid or hexafluoroisopropanol) to prepare a chitosan–gelatin-based nanofibrous mat (C8G8P2A0.5 mat), which has great potential for tissue engineering applications.

Acknowledgements

This study was financially supported by the National Science Council, Taiwan (grant numbers: NSC102-2221-E-002-162, NSC103-2221-E-002-209). The authors wish to express our gratitude to Yi-Hong Chou, Kai-Ping Chen, and Cuei-Fang Jhang for their contributions to this work.

References

Baker, R. W. (1987). *Controlled release of biologically active agents*. New York, NY: Wiley.
Bernardi, P., Scorrano, L., Colonna, R., Petronilli, V., & Di Lisa, F. (1999). Mitochondria and cell death—Mechanistic aspects and methodological issues. *European Journal of Biochemistry*, *264*(3), 687–701.
Busilacchi, A., Gigante, A., Mattioli-Belmonte, M., Manzotti, S., & Muzzarelli, R. A. A. (2013). Chitosan stabilizes platelet growth factors and modulates stem cell differentiation toward tissue regeneration. *Carbohydrate Polymers*, *98*(1), 665–676.
Chen, Z. G., Wang, P. W., Wei, B., Mo, X. M., & Cui, F. Z. (2010). Electrospun collagen–chitosan nanofiber: A biomimetic extracellular matrix for endothelial cell and smooth muscle cell. *Acta Biomaterialia*, *6*(2), 372–382.
Deitzel, J. M., Kleinmeyer, J., Harris, D., & Tan, N. C. B. (2001). The effect of processing variables on the morphology of electrospun nanofibers and textiles. *Polymer*, *42*(1), 261–272.
Desbrieres, J. (2002). Viscosity of semiflexible chitosan solutions: Influence of concentration, temperature, and role of intermolecular interactions. *Biomacromolecules*, *3*(2), 342–349.
Doshi, J., & Reneker, D. H. (1995). Electrospinning process and applications of electrospun fibers. *Journal of Electrostatics*, *35*(2–3), 151–160.
Geng, X. Y., Kwon, O. H., & Jang, J. H. (2005). Electrospinning of chitosan dissolved in concentrated acetic acid solution. *Biomaterials*, *26*(27), 5427–5432.
Haghi, A. K., & Akbari, M. (2007). Trends in electrospinning of natural nanofibers. *Physica Status Solidi a—Applications and Materials Science*, *204*(6), 1830–1834.
Hohman, M. M., Shin, M., Rutledge, G., & Brenner, M. P. (2001). Electrospinning and electrically forced jets. I. Stability theory. *Physics of Fluids*, *13*(8), 2201–2220.
Huang, Z. M., Zhang, Y. Z., Kotaki, M., & Ramakrishna, S. (2003). A review on polymer nanofibers by electrospinning and their applications in nanocomposites. *Composites Science and Technology*, *63*(15), 2223–2253.
Huang, Z. M., Zhang, Y. Z., Ramakrishna, S., & Lim, C. T. (2004). Electrospinning and mechanical characterization of gelatin nanofibers. *Polymer*, *45*(15), 5361–5368.
Hung, S. C., Yang, D. M., Chang, C. F., Lin, R. J., Wang, J. S., Ho, L. L. T., et al. (2004). Immortalization without neoplastic transformation of human mesenchymal stem cells by transduction with HPV16 E6/E7 genes. *International Journal of Cancer*, *110*(3), 313–319.
Jegal, J., & Lee, K. H. (1999). Nanofiltration membranes based on poly(vinyl alcohol) and ionic polymers. *Journal of Applied Polymer Science*, *72*(13), 1755–1762.
Kidoaki, S., Kwon, I. K., & Matsuda, T. (2005). Mesoscopic spatial designs of nano- and microfiber meshes for tissue-engineering matrix and scaffold based on newly devised multilayering and mixing electrospinning techniques. *Biomaterials*, *26*(1), 37–46.
Kiechel, M. A., & Schauer, C. L. (2013). Non-covalent crosslinkers for electrospun chitosan fibers. *Carbohydrate Polymers*, *95*(1), 123–133.

Le Trong, I., McDevitt, T. C., Nelson, K. E., Stayton, P. S., & Stenkamp, R. E. (2003). Structural characterization and comparison of RGD cell-adhesion recognition sites engineered into streptavidin. *Acta Crystallographica Section D—Biological Crystallography*, *59*, 828–834.

Ma, Z. W., He, W., Yong, T., & Ramakrishna, S. (2005). Grafting of gelatin on electrospun poly(caprolactone) nanofibers to improve endothelial cell spreading and proliferation and to control cell orientation. *Tissue Engineering*, *11*(7–8), 1149–1158.

Muzzarelli, R. A. A. (1977). *Chitin*. Amsterdam: Elsevier Science Limited.

Muzzarelli, R. A. A. (2011). Chitosan composites with inorganics, morphogenetic proteins and stem cells, for bone regeneration. *Carbohydrate Polymers*, *83*(4), 1433–1445.

Muzzarelli, R. A. A. (2012). 10.06—Nanochitins and nanochitosans, paving the way to eco-friendly and energy-saving exploitation of marine resources. In K. Matyjaszewski, & M. Möller (Eds.), *Polymer science: A comprehensive reference* (pp. 153–164). Amsterdam: Elsevier.

Muzzarelli, R. A. A., Boudrant, J., Meyer, D., Manno, N., DeMarchis, M., & Paoletti, M. G. (2012). Current views on fungal chitin/chitosan, human chitinases, food preservation, glucans, pectins and inulin: A tribute to Henri Braconnot, precursor of the carbohydrate polymers science, on the chitin bicentennial. *Carbohydrate Polymers*, *87*(2), 995–1012.

Nam, Y. S., Park, W. H., Ihm, D., & Hudson, S. M. (2010). Effect of the degree of deacetylation on the thermal decomposition of chitin and chitosan nanofibers. *Carbohydrate Polymers*, *80*(1), 291–295.

Phillips, G. O., & Williams, P. A. (2000). *Handbook of hydrocolloids*. Boca Raton, FL: CRC Press.

Reneker, D. H., & Chun, I. (1996). Nanometre diameter fibres of polymer, produced by electrospinning. *Nanotechnology*, *7*(3), 216–223.

Rosellini, E., Cristallini, C., Barbani, N., Vozzi, G., & Giusti, P. (2009). Preparation and characterization of alginate/gelatin blend films for cardiac tissue engineering. *Journal of Biomedical Materials Research A*, *91A*(2), 447–453.

Schiffman, J. D., & Schauer, C. L. (2007). Cross-linking chitosan nanofibers. *Biomacromolecules*, *8*(2), 594–601.

Shenoy, S. L., Bates, W. D., Frisch, H. L., & Wnek, G. E. (2005). Role of chain entanglements on fiber formation during electrospinning of polymer solutions: good solvent, non-specific polymer–polymer interaction limit. *Polymer*, *46*(10), 3372–3384.

Swenson, H. A., Kaustine, H. M., Kaustine, O. A., & Thompson, N. S. (1968). Structure of gum arabic and its configuration in solution. *Journal of Polymer Science A-2: Polymer Physics*, *6*(9), 1593–1606.

Tsai, C. C., Su, P. F., Huang, Y. F., Yew, T. L., & Hung, S. C. (2012). Oct4 and nanog directly regulate dnmt1 to maintain self-renewal and undifferentiated state in mesenchymal stem cells. *Molecular Cell*, *47*(2), 169–182.

Tsai, R.-Y., Chen, P.-W., Kuo, T.-Y., Lin, C.-M., Wang, D.-M., Hsien, T.-Y., et al. (2014). Chitosan/pectin/gum arabic polyelectrolyte complex: Process-dependent appearance, microstructure analysis and its application. *Carbohydrate Polymers*, *101*(0), 752–759.

Wang, X. F., Fang, D. F., Yoon, K., Hsiao, B. S., & Chu, B. (2006). High performance ultrafiltration composite membranes based on poly(vinyl alcohol) hydrogel coating on crosslinked nanofibrous poly(vinyl alcohol) scaffold. *Journal of Membrane Science*, *278*(1–2), 261–268.

Yuan, X. Y., Zhang, Y. Y., Dong, C. H., & Sheng, J. (2004). Morphology of ultrafine polysulfone fibers prepared by electrospinning. *Polymer International*, *53*(11), 1704–1710.

Zhu, X. L., Cui, W. G., Li, X. H., & Jin, Y. (2008). Electrospun fibrous mats with high porosity as potential scaffolds for skin tissue engineering. *Biomacromolecules*, *9*(7), 1795–1801.

Zong, X. H., Kim, K., Fang, D. F., Ran, S. F., Hsiao, B. S., & Chu, B. (2002). Structure and process relationship of electrospun bioabsorbable nanofiber membranes. *Polymer*, *43*(16), 4403–4412.